Scheme IV

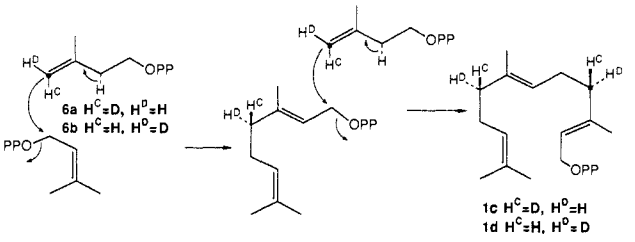


The proton that is lost from C-9 of **4** originates at C-8 of farnesyl pyrophosphate. To establish the stereochemical course of this deprotonation step, we prepared both (4*R*,8*R*)- and (4*S*,8*S*)-[4,8-$^2H_2$]FPP (**1c** and **1d**) by enzyme-catalyzed condensation of (4*Z*)- and (4*E*)-[4-$^2$H]isopentenyl pyrophosphate (**6a** and **6b**),[13,14] respectively, with dimethylallyl pyrophosphate in the presence of avian prenyl transferase[14,15] (Scheme IV). After incubation of each of the stereospecifically deuterated FPPs with aristolochene synthase, the resulting samples of aristolochene were analyzed by $^2$H NMR. As summarized in Scheme III, aristolochene **2c** (730 nmol) retained both deuterium atoms, as evidenced by the presence of signals at $\delta$ 1.44 and 5.35, corresponding to D-3a and D-9, while **2d** (500 nmol) showed a single peak at $\delta$ 1.36, corresponding to D-3b. These results demonstrate conclusively that it is H-8$_{si}$ that is lost in the formation of the 9,10-double bond of aristolochene.

On the basis of the known relative and absolute configuration of (+)-aristolochene,[3] it can be inferred that the sequential 1,2-hydride and methyl migrations take place on opposite faces of the bicyclic intermediate. Loss of H-8$_{si}$, which becomes H-9$\beta$ (H-9$_{si}$) in **4**, establishes that the proton that is lost must be syn to the migrating methyl group. The sequence of anti migration, syn deprotonation is readily explained by invoking a chair–boat conformation for the cyclizing FPP and intermediate germacrene A. Further experiments to test the proposed cyclization mechanism and to characterize the cyclase itself are in progress.

**Acknowledgment**. This work was supported by a grant from the National Institutes of Health, GM30301. We thank Dr. D. John Aberhart of the Worcester Foundation for Experimental Biology, Shrewsbury, MA, for a generous gift of stereospecifically deuterated 3-methylcrotonic acids, **5a** and **5b**. We also thank Steven W. Weiner for the preparation of [$^3$H]dimethylallyl pyrophosphate.

(10) Baker, F. C.; Brooks, C. J. W. *Phytochemistry* **1976**, *15*, 689. Baker, F. C.; Brooks, C. J. W.; Hutchinson, S. A. *J. Chem. Soc., Chem. Commun.* **1975**, 293.

(11) Birnbaum, G. I.; Huber, C. P.; Post, M. L.; Stothers, J. B.; Robinson, J. R.; Stoessl, A.; Ward, E. W. B. *J. Chem. Soc., Chem. Commun.* **1976**, 330.

(12) Threlfall, D. R.; Whitehead, I. M. *Phytochemistry* **1988**, *27*, 2567. Whitehead, I. M.; Threlfall, D. R.; Ewing, D. F. *Phytochemistry* **1989**, *28*, 775. Vogeli, U.; Chappel, J. *Plant Physiol.* **1988**, *88*, 1291. Whitehead, I. M.; Prabhakaran, P. C.; Ewing, D. F.; Cane, D. E.; Threllfall, D. R. *Phytochemistry* **1990**, *29*, 479.

(13) Ogura, K.; Koyama, T.; Kobayashi, M.; Ito, M. *Biochemistry* **1987**, *26*, 4745.

(14) Cane, D. E.; McIlwaine, D. B.; Oliver, J. S. *J. Am. Chem. Soc.* **1990**, *112*, 1285.

(15) The ionization–condensation–elimination reaction has been shown to take place on the *re* face of the isopentyl pyrophosphate double bond.[16] A typical incubation involved 20 $\mu$mol of (4*Z*)-[4-$^2$H]isopentenyl pyrophosphate, 0.46 $\mu$Ci of [4-$^{14}$C]isopentenyl pyrophosphate, and 20 $\mu$mol of [1-$^3$H]dimethylallyl pyrophosphate in 6.8 mL of 20 mM Tris buffer, pH 7.7, containing 10 mM $MgCl_2$, 7 mM DTE, and 508 units of avian prenyl transferase which had been purified from chicken livers to the hydroxy apatite step [specific activity 14 nmol min$^{-1}$ (mg of protein)$^{-1}$] (Reed, B. C.; Rilling, H. C. *Biochemistry* **1975**, *14*, 50). After 12 h at 30 °C, the resulting **1c** was purified by a sequence of Sephadex G-25 gel filtration, $C_{18}$ reverse-phase ion pairing, and DEAE-Sephadex ion-exchange chromatography, to yield 1.3 $\mu$mol of (4*R*,8*R*)-[4,8-$^2H_2$]FPP.[14,17]

(16) Cornforth, J. W.; Cornforth, R. H.; Popjak, G.; Yengoyan, L. *J. Biol. Chem.* **1966**, *241*, 3970. Donninger, C.; Popjak, G. *Proc. R. Soc. London, B* **1966**, *163*, 465. Cornforth, J. W.; Cornforth, R. H.; Donninger, C.; Popjak, G. *Proc. R. Soc. London, B* **1966**, *163*, 492. Popjak, G.; Cornforth, J. W. *Biochem. J.* **1966**, *101*, 553.

(17) Cane, D. E.; Oliver, J. S.; Harrison, P. H. M.; Abell, C.; Hubbard, B. R.; Kane, C. T.; Lattman, R. *J. Am. Chem. Soc.*, in press.

# Tetrahedral Copper(II) Complexes Supported by a Hindered Pyrazolylborate. Formation of the Thiolato Complex, Which Closely Mimics the Spectroscopic Characteristics of Blue Copper Proteins

Nobumasa Kitajima,* Kiyoshi Fujisawa, and Yoshihiko Moro-oka*

*Research Laboratory of Resources Utilization*
*Tokyo Institute of Technology*
*4259 Nagatsuta, Midori-ku, Yokohama 227, Japan*

*Received September 14, 1989*

Synthetic examples of tetrahedral copper(II) complexes are rare, despite current interest in their unusual electronic structure from both physicochemical and biological points of view.[1] We now report that a hindered tripod nitrogen ligand,[2] HB(3,5-i$Pr_2$pz)$_3^-$, stabilizes the tetrahedral coordination geometry with reasonable durability in the solid state or in noncoordinating solvents.

The reaction of KHB(3,5-i$Pr_2$pz)$_3$ with 1 equiv of $CuCl_2 \cdot 2H_2O$ in dry acetone gives Cu(Cl)(HB(3,5-i$Pr_2$pz)$_2$) (**1**) as a deep brown microcrystalline solid in 60–70% yield.[3] The same reaction with KHBpz$_3$ and KHB(3,5-$Me_2$pz)$_3$ yields only the disproportionation products, Cu(HBpz$_3$)$_2$[4] and Cu(HB(3,5-$Me_2$pz)$_3$)$_2$,[5] respectively. The crystal structure of **1** is shown in Figure 1.[6] The copper, chlorine, boron, and one pyrazole ring lie on a crystallographically imposed mirror plane. The mean bond lengths of Cu–Cl and Cu–N are close to one another, 2.13–1.98 Å, with the dihedral angles approximately 90°. Hence, the coordination geometry of **1** is described as a tetrahedron that is slightly elongated toward the chlorine atom. Although several examples[7] of tetrahedral copper(II) complexes have been reported, their dihedral angles are not comparable to 90°, but lie in the range 50–70°, owing to significant flattening or elongation.

The absorption spectrum of a solution of **1** in a noncoordinating solvent ($CH_2Cl_2$, toluene, or pentane) is essentially identical with the reflectance spectrum of the solid sample of **1**, implying that the tetrahedral structure is preserved in these solvents. However, addition of a slight amount of a coordinating solvent such as DMSO and DMF into a $CH_2Cl_2$ solution of **1** causes the immediate formation of the solvent adduct. The DMF adduct Cu(Cl)(DMF)(HB(3,5-i$Pr_2$pz)$_3$) (**3**) was isolated, and the structure was established by X-ray crystallography.[8] As shown in Figure 2, the adduct is a pentacoordinated complex of square-pyramidal geometry with one pyrazole nitrogen as an apical ligand. Owing to the formation of the adduct, the d–d band of

(1) (a) Yokoi, H.; Addison, A. W. *Inorg. Chem.* **1977**, *6*, 1341. (b) Gewirth, A. A.; Cohen, S. L.; Schugar, H. J.; Solomon, E. I. *Ibid.* **1987**, *26*, 1133. (c) Gewirth, A. A.; Solomon, E. I. *J. Am. Chem. Soc.* **1988**, *110*, 3811.

(2) Kitajima, N.; Fujisawa, K.; Fujimoto, C.; Moro-oka, Y. *Chem. Lett.* **1989**, 421.

(3) Anal. Calcd for $C_{27}H_{46}N_6BCuCl$: C, 57.45; H, 8.21; N, 14.89; Cl, 6.28. Found for crystals of **1**: C, 57.03; H, 8.06; N, 14.82; Cl, 6.12. IR (KBr, cm$^{-1}$): 2545 (BH). UV-vis [$\lambda_{max}$, nm ($\epsilon$, cm$^{-1}$ M$^{-1}$)]: (in $CH_2Cl_2$) 996 (150), 510 (310), 362 (1900), 262 (1600); (in DMF) 758 (100), 530 (80), 346 (1100), 269 (4400). The reaction with $CuBr_2$ gave Cu(Br)(HB(3,5-i$Pr_2$pz)$_3$) (**2**). Calcd for $C_{27}H_{46}N_6BCuBr$: C, 53.25; H, 7.61; N, 13.80; Br, 13.12. Found for **2**: C, 53.36; H, 7.72; N, 13.74; Br, 13.09.

(4) Murphy, A.; Hathaway, B. J.; King, T. J. *J. Chem. Soc., Dalton Trans.* **1979**, 1646.

(5) Kitajima, N.; Moro-oka, Y.; Uchida, A.; Sasada, Y.; Ohashi, Y. *Acta Crystallogr.* **1988**, *C44*, 1876.

(6) **1** crystallizes in space group $P2_1/m$ with $a$ = 10.039 (1) Å, $b$ = 16.519 (3) Å, $c$ = 9.868 (2) Å, $\beta$ = 102.60 (1)°, $V$ = 1597.1 (4) Å$^3$, and $D_{calcd}$ = 1.18 g cm$^{-1}$ for $Z$ = 2. Full-matrix least-squares refinement of the model based on 1093 reflections ($F_o > 3\sigma(F_o)$) converged to a final $R$ = 8.03% and $R_w$ = 7.93%. All non-hydrogen atoms were refined anisotropically. Hydrogen atoms except for the ones on the methyl groups were calculated and fixed in the refinement ($d$(C–H) = 1.0 Å).

(7) Knapp, S.; Keenan, T. P.; Zhang, X.; Fikar, R.; Potenza, J. A.; Schugar, H. J. *J. Am. Chem. Soc.* **1987**, *109*, 1882 and references cited therein.

(8) Anal. Calcd for $C_{30}H_{53}N_7BOCuCl$: C, 56.51; H, 8.38; N, 15.38; Cl, 5.56. Found for crystals of **3**: C, 56.50; H, 8.70; N, 15.16; Cl, 5.82. IR (KBr, cm$^{-1}$): 2543 (BH) 1640 (CO). **3** crystallizes in space group $P2_1/a$ with $a$ = 27.252 (4) Å, $b$ = 14.103 (2) Å, $c$ = 9.469 (1) Å, $\beta$ = 96.99 (1)°, $V$ = 3612.4 (9) Å$^3$, and $D_{calcd}$ = 1.20 g cm$^{-1}$ for $Z$ = 4. For 5283 independent reflections with $F_o > 3\sigma(F_o)$, the final $R$ = 7.98% and $R_w$ = 6.63%.

0002-7863/90/1512-3210$02.50/0 

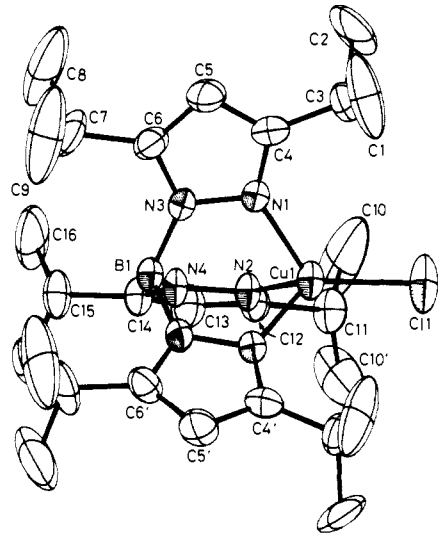


**Figure 1.** ORTEP drawing of $Cu(Cl)(HB(3,5\text{-}iPr_2pz)_3)$ (**1**). Selected bond distances (Å) and angles (deg): Cu1–Cl1, 2.125 (6); Cu1–N1, 1.980 (13); Cu1–N2, 1.985 (11); Cl1–Cu1–N1, 122.9 (3); Cl1–Cu1–N2, 125.3 (5); N1–Cu1–N2, 92.1 (4). Dihedral angles (deg): N1–Cu1–N2/N1′–Cu1–Cl1, 89.89; N1–Cu1–N1′/Ni–Cu1–Cl1, 90.00; N1–Cu1–Cl1/N2–Cu1–N1′, 90.12.

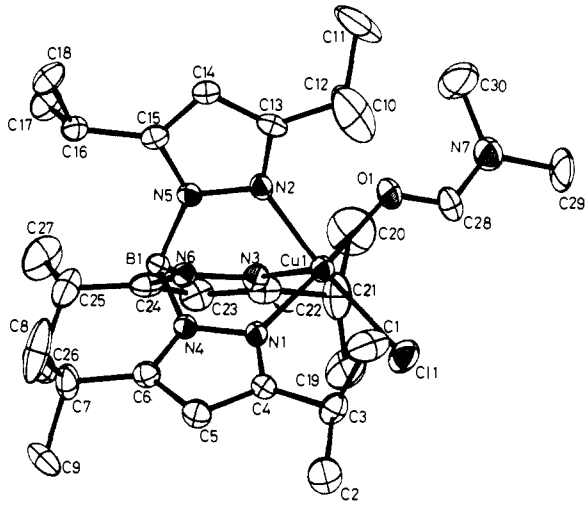


**Figure 2.** ORTEP drawing of $Cu(Cl)(DMF)(HB(3,5\text{-}iPr_2pz)_3)$ (**3**). Selected bond distances (Å) and angles (deg): Cu1–N1, 2.041 (6); Cu1–N2, 2.027 (5); Cu1–N3, 2.184 (6); Cu1–O1, 2.063 (5); Cu1–Cl1, 2.260 (2); N3–Cu1–N1, 92.3 (2); N3–Cu1–N2, 90.8 (2); N3–Cu1O1, 94.8 (2); N3–Cu1–Cl1, 101.9 (2).

**Scheme I**

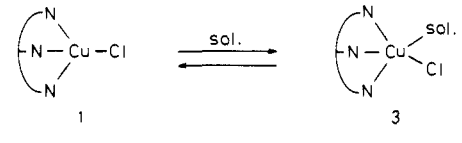


**1** at 996 nm in $CH_2Cl_2$ is shifted to 758 nm in DMF and the EPR spectrum changes drastically as shown in Figure 3. The spectrum of **1** obtained in $CH_2Cl_2$ shows the reverse signal (spectrum A), which implicates the characteristic electronic state of **1**, the $d_{z^2}$ ground state, as predicted from the coordination structure. On the other hand, the spectrum obtained in DMF exhibits an axially symmetric signal typical for a square-pyramidal copper(II) complex (spectrum B). In THF or acetone, **1** does not form the adduct at room temperature; however, below −78 °C, the color of the solution turns green and the frozen solution in liquid nitrogen shows an axial EPR signal ascribed to the formation of the pentacoordinated adduct (Scheme I).

Previously, with $HB(3,5\text{-}Me_2pz)_3^-$ as a ligand, efforts were made to prepare a tetrahedral thiolato copper(II) complex to mimic the

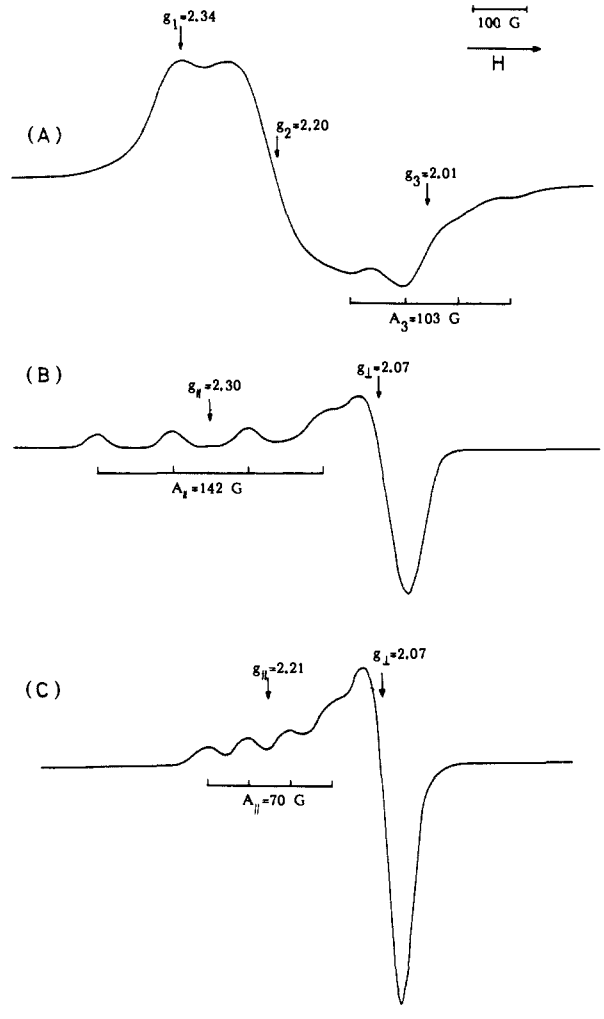


**Figure 3.** EPR spectra of mononuclear copper(II) complexes ligated by $HB(3,5\text{-}iPr_2pz)_3^-$ at 77 K: (A) $Cu(Cl)(HB(3,5\text{-}iPr_2pz)_3)$ (**1**) in $CH_2Cl_2$; (B) **1** or $Cu(Cl)(DMF)(HB(3,5\text{-}iPr_2pz)_3)$ (**3**) in DMF; (C) $Cu(StBu)(HB(3,5\text{-}iPr_2pz)_3)$ (**5**) in $CH_2Cl_2$.

**Scheme II**

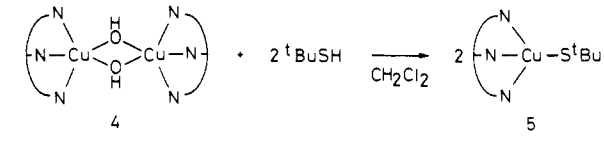


physicochemical characteristics of blue copper proteins.[9] Although the *p*-nitrobenzenethiolato complex obtained showed a strong absorption band at 588 nm assignable to a S → Cu LMCT band, the EPR spectrum ($g_\parallel$ = 2.29, $g_\perp$ = 2.07, $A_\parallel$ = 160 G) was not similar to those of blue copper proteins. Rather, it resembled those of tetragonal copper(II) complexes. The formation of the pentacoordinated solvent adduct of **1**, as described above, prompted us to reconsider the experimental result since the synthesis was accomplished in THF. In order to prevent formation of the solvent adduct, we attempted the preparation of the tetrahedral thiolato copper(II) complex in $CH_2Cl_2$ with the present hindered pyrazolylborate. Although the reaction of **1** with NaSR in $CH_2Cl_2$ resulted in the reduction of **1**, the reaction of $Cu[HB(3,5\text{-}iPr_2pz)_3]_2(OH)_2$[10] (**4**) with 2 equiv of tBuSH was found to proceed smoothly at −20 °C (Scheme II). The resulting deep-blue solution showed a strong absorption band at 608 nm ($\epsilon$, ≥3500, at −16 °C) and also gave rise to an unusual EPR signal that is similar to those of blue copper proteins (Figure 3C).[11] Although the

(9) (a) Thompson, J. S.; Marks, T. J.; Ibers, J. A. *Proc. Natl. Acad. Sci. U.S.A.* **1977**, *74*, 3114. (b) Thompson, J. S.; Marks, T. J.; Ibers, J. A. *J. Am. Chem. Soc.* **1979**, *101*, 4180.

(10) Kitajima, N.; Fujisawa, K.; Moro-oka, Y. *Inorg. Chem.* In press.

redox[12] potential (-540 mV vs Ag wire at -20 °C in $CH_2Cl_2$ under argon) is considerably lower than those of blue copper proteins, the present experimental result clearly proves that the striking spectroscopic characteristics of blue copper proteins (a strong absorption band at ca. 600 nm ($\epsilon$, 1500–5000) and an unusually small hyperfine constant ($A_\parallel \leq 70$ G)) can be mimicked by a simple synthetic model, a tetrahedral thiolato copper(II) complex in the absence of the coordination of a thioether.[13]

**Acknowledgment**. We thank Dr. R. Makino and Prof. Y. Ishimura of Keio University for low-temperature measurements of electronic spectra. Support of this work by a Grant-in-Aid for Scientific Research from the Japanese Ministry of Education, Science and Culture (62430018 and 01607003) and by Kawakami Memorial Foundation is gratefully acknowledged.

**Registry No.** 1, 125782-21-0; 2, 124688-39-7; 3, 125782-22-1; 4, 123676-54-0; 5, 125782-23-2.

**Supplementary Material Available:** Tables S-I–S-V of the summary of X-ray analyses, atomic coordinates, anisotropic thermal parameters, and bond distances and angles for 1 and 3 (19 pages); Table S-VI listing observed and calculated structure factors for 1 and 3 (19 pages). Ordering information is given on any current masthead page.

(11) Other absorption bands of 5 are observed at 349 nm ($\epsilon$, ~11 000) and ≳900 nm (~500). Because of the very high solubility, complex 5 has not been isolated as a crystalline solid so far. However, the quantitative measurement of the EPR signal led us to the conclusion that the reaction of 4 and tBuSH proceeds quantitatively (since the binuclear hydroxo complex 4 is EPR silent, the measurement is accurate). The details of the properties and structure of 5 will be described elsewhere.

(12) The completely reversible redox couple of the thiolato complex is indicative of considerable stability of the reduced state. We infer that the structure is identical with that of a tetrahedral thiolato copper(I) complex reported by Marks et al.[9]

(13) (a) Sugiura, Y.; Hirayama, Y. *J. Am. Chem. Soc.* **1977**, *99*, 1581. (b) Bharadwaj, P. K.; Potenza, J. A.; Schugar, H. J. *Ibid.* **1986**, *108*, 1351. (c) Anderson, O. P.; Becher, J.; Frydendahl, H.; Taylor, L. F.; Toftlund, H. *J. Chem. Soc., Chem. Commun.* **1986**, 699.

## Intact Incorporation of Acetate-Derived Di- and Tetraketides during Biosynthesis of Dehydrocurvularin, a Macrolide Phytotoxin from *Alternaria cinerariae*

Yuko Yoshizawa, Zhe Li, Paul B. Reese,† and John C. Vederas*

*Department of Chemistry, University of Alberta Edmonton, Alberta, Canada T6G 2G2*

*Received November 9, 1989*

Extensive studies with simple precursors (e.g., acetate, propionate) labeled with stable isotopes support the hypothesis that polyketide biosynthesis resembles fatty acid formation except that particular reductive steps are absent during assembly of the carbon chain.[1,2] This results in incorporation of keto, hydroxy, or olefinic functionality in the growing enzyme-bound polyketide that can lead to further transformations (e.g., cyclization) or provide sites for post-assembly processing (e.g., oxidation, alkylation) by other enzymes.[3,4] Key support for this proposal is provided by recent experiments in which functionalized propionate-derived di- or

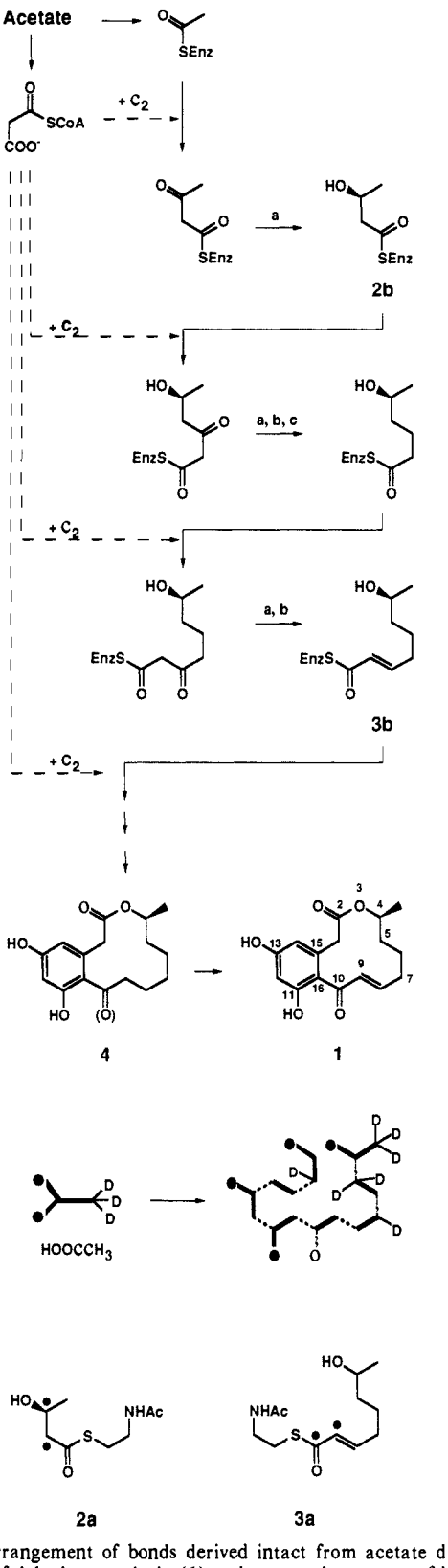


**Figure 1.** Arrangement of bonds derived intact from acetate during biosynthesis of dehydrocurvularin (1) and proposed sequence of its assembly by a polyketide synthase. In between each addition of two carbons (+$C_2$) from malonyl-CoA (with $CO_2$ loss), functionality changes can occur: (a) reduction of β-hydroxy thiol ester; (b) dehydration to α,β-unsaturated thiol ester; (c) reduction to saturated thiol ester.

†NSERC CIDA Fellow. Permanent address: Department of Chemistry, University of the West Indies at Mona, Kingston, Jamaica.

(1) (a) Vederas, J. C. *Nat. Prod. Rep.* **1987**, *4*, 277–337. (b) Simpson, T. J. *Chem. Soc. Rev.* **1987**, *16*, 123–160. (c) Simpson, T. J. *Nat. Prod. Rep.* **1987**, *4*, 339–376. (d) O'Hagan, D. *Nat. Prod. Rep.* **1989**, *6*, 205–219.

(2) (a) Rawlings, B. J.; Reese, P. B.; Ramer, S. E.; Vederas, J. C. *J. Am. Chem. Soc.* **1989**, *111*, 3382–3390. (b) Arai, K.; Rawlings, B. J.; Yoshizawa, Y.; Vederas, J. C. *J. Am. Chem. Soc.* **1989**, *111*, 3391–3399. (c) Ashworth, D. M.; Clark, C. A.; Robinson, J. A. *J. Chem. Soc., Perkin Trans. 1* **1989**, 1461–1467.

(3) Addition of oxygenase inhibitors to polyketide fermentations can yield deoxy compounds that presumably resemble the product initially produced by the synthase enzyme complex: Oikawa, H.; Ichihara, A.; Sakamura, S. *J. Chem. Soc., Chem. Commun.* **1988**, 600–602.

0002-7863/90/1512-3212$02.50/0 